Cement and Concrete Research 148 (2021) 106534

Contents lists available at ScienceDirect

Cement and Concrete Research

journal homepage: www.elsevier.com/locate/cemconres

Effects of carbonation on the retention of heavy metals in chemically activated BOF slag pastes

A.M. Kaja [a], A. Delsing [a], S.R. van der Laan [a,b], H.J.H. Brouwers [a], Qingliang Yu [a,c,*]

[a] Department of the Built Environment, Eindhoven University of Technology, Eindhoven, 5600, MB, the Netherlands
[b] Tata Steel, R&D, Microstructure & Surface Characterization (MSC), P.O. Box 10.000, 1970 CA IJmuiden, the Netherlands
[c] School of Civil Engineering, Wuhan University, 430072 Wuhan, PR China

ARTICLE INFO

Keywords:
BOF slag
Citrate salt
Hydration
Carbonation
Leaching

ABSTRACT

Basic Oxygen Furnace slag contains heavy metals, including vanadium, chromium and molybdenum. The leachability of these elements determines the industrial applicability of slag-based building products. This study investigates the post-carbonation leaching of heavy metals from activated BOF slag pastes with the focus on the activator dosage and type (sodium and potassium citrate). Results reveal that the high degree of brownmillerite hydration boosts the leachability of heavy metals as its hydration product- hydrogarnet is less stable upon carbonation. With two leaching procedures, it is demonstrated that the carbonation resistance of pastes becomes the main attribute in preventing the leaching of heavy metals. It can be enhanced by optimising the activator dosage to facilitate the hydration of C_2S and consequent structural densification.

1. Introduction

Current worldwide steel production reaches ~1.8 billion tons per year [1], among which about 2/3 is produced via the Basic Oxygen Steelmaking (BOS) process [2]. With this method, per ton of steel, 90–110 kg of Basic Oxygen Furnace (BOF) slag are generated [3,4]. Therefore, vast quantities of BOF slag are available for reuse in the industry. Even though concrete technology offers a promising field for BOF slag utilisation, its application as a binder constituent seems thus far precluded, mainly due to contamination with heavy metals and low reactivity [5,6].

The chemical/mineralogical composition of BOF slag varies depending on the raw materials and process parameters used during the steel production. Nonetheless, it is generally represented by C_2S, C_3S, $C_2(A,F)$, RO phase (CaO-FeO-MgO-MnO solid solution, with the wuestite structure), and free CaO [7,8]. Among these phases, C_2S and $C_2(A,F)$ are potentially the most reactive, but at the same time, they are reported to be the host phases for vanadium and $C_2(A,F)$ also for chromium [9–12].

In order to evaluate the hazardous impact of BOF slag on the environment, many studies focus on the leaching of heavy metals from the original material. In general, it is shown that non-weathered slags release relatively low quantities of vanadium and chromium [10,13,14]. According to Chaurand et al. [12,15], in BOF slag, chromium is present as Cr(III) (octahedral coordination), which is less mobile and less toxic than Cr(VI) and remains at this oxidation state during leaching. In consequence, the release of Cr from BOF slag is minor. The leaching values of vanadium are usually higher than those of chromium. Nonetheless, they often fall below the standardised limits for heavy metals leaching [16], as at highly alkaline conditions (e.g. in the presence of portlandite), vanadium is relatively immobile [3].

The weathering, however, greatly affects the release of heavy metals from BOF slags. Costa et al. [17] showed that while leaching of chromium remains the same or becomes slightly reduced after carbonation, leaching of vanadium from carbonated slag can increase even 500 times. In BOF slag, vanadium predominately prevails at V(IV) and V(V) [12,18]. However, during natural ageing, V(IV) is oxidised to V(V), being the most toxic oxidation state [12,15]. Significant release of vanadium from BOF slag after carbonation coincidences mainly with the pH drop caused by the reaction of portlandite with CO_2 [2].

The leaching behaviour of the non-hydrated, loose slag powder cannot be directly transferred to the leaching behaviour of slag-based shaped building materials. In our previous work [10,19], we showed that the problem of low reactivity of slag could be overcome with the addition of tri-potassium citrate. Chemical activation significantly enhances the hydration of BOF slag, and as a consequence, high-end performance building products can be manufactured. In the proposed

* Corresponding author.
E-mail address: q.yu@bwk.tue.nl (Q. Yu).

https://doi.org/10.1016/j.cemconres.2021.106534
Received 10 November 2020; Received in revised form 29 June 2021; Accepted 5 July 2021
Available online 13 July 2021

activation process, the reaction of the most contaminated phases-brownmillerite and belite takes place, resulting in the formation of siliceous hydrogarnet and C-S-H gel [10]. These hydration products are known to reveal high capacities for heavy metals immobilisation. Hydroandradites $Ca_3(Al_xFe_{1-x})_2(SiO_4)_y(OH)_{4(3-y)}$, belonging to the hydrogarnet group, can incorporate heavy metals in their structure by substituting aluminum/iron in octahedral positions or hydroxyls ($H_4O_4^{4-}$) in tetrahedral positions. Accordingly, in hydrogarnets, chromium (III) substitutes iron/aluminum [20], and chromium (VI), in the form of oxyanions (chromate (CrO_4^{2-})), substitutes hydroxyls [21]. With a similar size as chromium oxyanions, vanadium oxyanions (VO_4^{3-}) could also potentially replace the hydroxyls in hydrogarnets structure. However, this would require charge balancing. Vollpracht et al. [22] suggested that in hydrating cement, vanadium oxyanions are adsorbed on the C-S-H gel. Immobilisation of chromium in C-S-H gel by means of Si substitution is also sometimes proposed [23–25].

The high immobilisation potential of BOF slag hydration products was confirmed in our previous study with a leaching test [10]. Well-sealed samples of chemically activated BOF slag did not reveal leaching problems even though the phases containing heavy metals underwent hydration. However, similarly as observed in the raw BOF slag, the carbonation of hydration products can lead to the increased release of heavy metals. Upon carbonation, changes in the phase composition occur and are accompanied by a significant pH reduction. The C-S-H gel and hydroandradite (phases that are potentially hosting heavy metals in the hydrated BOF slag) are known to undergo carbonation. The reaction of C-S-H gel with CO_2 leads to the formation of calcite and amorphous silica [26,27]. Carbonation of hydrogarnets also takes place, as predicted with thermodynamic modeling [28]. The data are, however, limited and mainly focused on the carbonation of Al-based hydrogarnets.

Regarding the release of heavy metals from the shaped BOF slag-based products, carbonation resistance, defined as the depth where the compositional changes and the drop of pH occur, may become a crucial factor controlling the applicability of these materials. Therefore, the extent and impact of carbonation on the leaching of heavy metals need to be evaluated, considering not only the release of heavy metals from the dissolving phases but also the possibility of their further immobilisation in the newly formed carbonation products.

Following the above discussion, in this study, we focus on the hydration of newly designed chemically activated BOF slag-based materials and their resistance to carbonation in order to evaluate the retention of heavy metals during their service life. For the representativeness of this study, two types of citrate-based activators (with varying concentrations) and two leaching procedures are employed. To account for the chemical and physical factors affecting the release of heavy metals, the leaching from unshaped and shaped slag pastes is analysed before and after carbonation in the context of reactivity of the slag phases, hydration products, carbonation resistance of pastes and compositional changes induced by the carbonation. The results demonstrate that the leaching of heavy metals from BOF slag pastes increases significantly after carbonation, mainly due to the decomposition of hydrogarnets and C-S-H gel. Nevertheless, our observations show that this effect can be minimised by optimising the initial mix design. Higher hydration degrees of C_2S after 90 days of curing in pastes with 0.1 M and 0.2 M solutions of citrate salts than in pastes with more concentrated solutions lead to microstructural densification and consequent improvement of the carbonation resistance.

2. Experimental

2.1. Materials

The Basic Oxygen Furnace (BOF) slag from Tata Steel (The Netherlands) was used as the raw material. The slag was ground prior to the application. The particle size distribution is shown in Fig. 1, as measured with laser diffraction spectroscopy (Mastersizer 2000, Malvern).

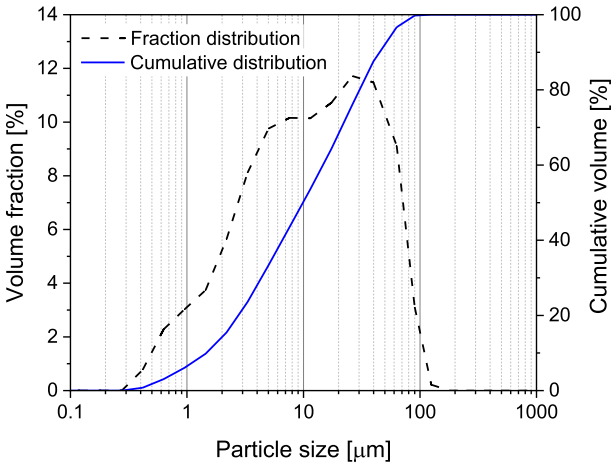

Fig. 1. The particle size distribution of BOF slag.

The chemical and mineralogical compositions were determined respectively with X-ray fluorescence (XRF) and X-ray diffraction (XRD) with quantitative Rietveld refinement, as described in more detail in the methodology section. The results are presented in Table 1. Polymorphs of C_2S are reported combined with a single value.

The distribution of heavy metals within the BOF slag phases is determined with electron probe microanalysis (EPMA). The EPMA measurements were performed using a Cameca SX 100 microprobe with five vertical spectrometers. An accelerating voltage of 15 kV and a beam current of 200 nA were applied. The spot size was kept as small as possible, ~1 μm. The peak measurement time for Mg, Al, Si, P, Ca, Ti, Cr, Mn was 60 s; and for V, Fe was 30 s. Background measurement time equal to half of the peak measurement time was used on each side of the peak. The following analysing crystals were used: LTAP (Mg, Al, Si), LPET (P, Ti, V), PET (Ca), LLiF (Cr, Mn, Fe). A minimum of 19 points per phase was analysed on 10 different slag fragments. The results are presented in Table 2.

Potassium and sodium salts of citric acid were applied in this study to activate the BOF slag phases. Technical grade products, tri-potassium citrate monohydrate ($K_3C_6H_5O_7{\cdot}H_2O$) and tri-sodium citrate dihydrate ($Na_3C_6H_5O_7{\cdot}2H_2O$), both with >99% purity, were used.

2.2. Methodology

2.2.1. Mix design and sample preparation

Two series of BOF slag pastes with increasing content of sodium and potassium citrate were prepared and analysed in this study. The concentrations of the citrate salts were selected based on our previous work [19]. Water to binder ratio (w/b) of 0.18 was applied for all mixtures. The detailed mix proportions are presented in Table 3. The activators

Table 1
Oxide and phase composition of BOF slag.

Mineral compound	Content [wt%]	Oxide	Content [wt%]
Brownmillerite	21.6	MgO	6.0
Magnetite	11.3	SiO_2	11.9
C_2S	32.1	Al_2O_3	3.2
Wuestite	20.6	CaO	41.0
Lime	1.1	P_2O_5	1.4
Calcite	0.3	TiO_2	1.1
Portlandite	0.5	V_2O_5	1.1
C_3S	0.9	Cr_2O_3	0.3
Amorphous	11.6	MnO	4.7
		Fe_2O_3	29.1
		GOI 1000	0.01

Table 2
Chemical composition of the phases containing heavy metals, derived from EPMA analyses (wt%) including the 1 sigma variation for the elements of interest, Cr and V.

Mineral	MgO	Al_2O_3	SiO_2	P_2O_5	CaO	TiO_2	V_2O_3	σ	Cr_2O_3	σ	MnO	FeO (Fe_2O_3*)	Total
C_2S	0.2	0.9	28.9	3.8	61.5	0.6	0.8	*0.4*	0.0	*0.0*	0.2	1.1	97.9
Wuestite	24.5	0.2	0.0	0.0	2.5	0.0	0.1	*0.1*	0.8	*0.3*	11.9	59.1	99.2
Brownmillerite	4.0	9.2	4.3	0.4	40.3	5.2	1.7	*0.8*	0.7	*0.7*	2.3	31.4*	99.4

Table 3
Mix design of the BOF slag pastes.

Sample description	BOF slag [g]	Water [g]	Tri-potassium citrate monohydrate [M]	Tri-sodium citrate dihydrate [M]	w/b	Flowability [mm]
K0.1	100	18	0.1		0.18	160
K0.2	100	18	0.2		0.18	240
K0.4	100	18	0.4		0.18	250
K0.6	100	18	0.6		0.18	280
Na0.1	100	18		0.1	0.18	150
Na0.2	100	18		0.2	0.18	200
Na0.4	100	18		0.4	0.18	220
Na0.6	100	18		0.6	0.18	250

were firstly dissolved in water to obtain the designed molarity. Solutions were subsequently mixed with slag powder using a high-speed mixer for 3 min.

Owing to the superplasticizing properties of citrate salts and a broad range of concentrations investigated in this study, slight bleeding was observed for the samples with the high activator dosages. This, however, did not have a substantial impact on the results, as revealed e.g. with the compressive strength test. The water amount was kept fixed as the spacing factor plays a vital role in the hydration of the C_2S phase [29]. The flowability of pastes, measured using a Hägermann cone, is presented in Table 3.

2.2.2. Evaluation of the hydration process

2.2.2.1. Isothermal calorimetry. The heat release during the first 7 days of hydration of BOF slag pastes was monitored with an isothermal conduction calorimeter (TAM Air, Thermometric). Pastes were externally mixed for 2 min and then loaded into the calorimeter. The data were recorded and analysed between 45 min and 160 h.

2.2.2.2. Early age solutions analyses. The early age solutions were extracted from the pastes after 30 and 60 min of hydration with pressure filtration. In order to remove possibly remaining solids, the solutions were subsequently filtered through a 0.22 μm membrane filter before the analyses. The concentration of OH^- was determined via titration against hydrochloride acid (0.1 mol/l), as described in [30]. The solutions were analysed with an ion chromatograph (Thermo scientific Dionex 1100), and after acidification with concentrated HNO_3, with inductively coupled plasma atomic emission spectrometer (ICP-OES, SPECTROBLUE). The multi-element standards IV and VI from Merck were used for the calibrations.

The concentration of citrates was determined with an ion chromatograph equipped with an ion-exchange column AS9-HS (2 × 250 mm). The 25 mM sodium carbonate (Na_2CO_3)/12 mM sodium bicarbonate ($NaHCO_3$) was used as an eluent. Citrate ions were detected via suppressed conductivity (Thermo scientific Dionex AERS 500, 2 mm). The external standards for the calibration (200, 100, 50, 20, 10, 5, 2,1 and 0.5 mg/l) were prepared from the citrate standard for IC (Merck, 1000 ± 5 mg/l).

2.2.2.3. Thermogravimetry. The amount of chemically bound water was determined with the thermogravimetric method. The hydration stoppage was carried out applying the double solvent exchange method, comprising of 30 min soaking in isopropanol, flushing with diethyl ether and semi-vacuum drying at 40 °C for 8 min. The powders were heated up from 40 to 1000 °C using a Jupiter STA 449 F1 Netzsch instrument with a heating rate of 5 °C/min, under a nitrogen flow of 20 ml/min.

2.2.2.4. X-ray diffraction. Changes in the phase composition of hydrating BOF slag were analysed based on X-ray diffraction patterns, with the XRD Rietveld method after 7, 28 and 90 days of hydration. Prior to the analyses, the hydration was stopped with the double solvent exchange method. The powders were milled in an XRD-Mill McCrone (RETSCH) and backloaded into the sample holders. The D4 ENDEAVOR X-ray diffractometer with CoKα radiation was used to collect the XRD patterns. The powders were scanned with a LynxEye detector in the range between 12 and 80° 2θ with a step size of 0.014° 2θ and a time per step of 1 s. The obtained diffractograms were analysed with TOPAS Academic software v5.0 with the fundamental parameter approach. The external standard method (corundum standard) was employed for phase quantification [31]. The crystal structures used for the Rietveld refinement are catalogued in Table 4 while described in detail in [19]. The lattice and microstrain parameters refined on the anhydrous slag were used for the analyses of the pastes.

2.2.2.5. Compressive strength. For the evaluation of mechanical performance, pastes were cast in cubic moulds (4 × 4 × 4 cm^3), vibrated for 2 min, and covered with foil to prevent evaporation of water and carbonation. After 24 h of curing, they were demoulded, sealed with foil, and transferred to the climate chamber (20 °C, RH > 95%). After designed curing ages, the compressive strength was evaluated according to EN 196-1 [32].

2.2.3. Carbonation resistance and heavy metals retention

To evaluate the post-carbonation leaching behaviour, the leaching

Table 4
The crystal structures of the phases used for the Rietveld refinement [19].

Phase	ICSD
Brownmillerite	9197
α′-C_2S	81,097
Wuestite	67,200
C_3S	64,759
β-C_2S	245,074
Magnetite	20,596
Lime	28,905
Portlandite	202,220
Hydrogarnet	29,247
Katoite	9272
Pyroaurite	6295

tests were performed on hydrated BOF slag pastes before and after carbonation curing. Two leaching tests were selected, the tank leaching test (NEN 7375:2004) [33] and the one batch leaching test (EN 12457-2) [34]. The BOF slag pastes were prepared with the same procedure as for the compressive strength determination. The first series of pastes (for the tank test) was cast in cubic moulds ($4 \times 4 \times 4$ cm^3) and covered with foil to prevent moisture loss and carbonation. After 24 h, samples were demoulded and sealed with foil and adhesive tape. The second series of pastes (for the one batch leaching test) was cast in cylindrical polyethylene vessels sealed with parafilm. All the samples were cured in the climate chamber (20 °C, RH > 95%) for 90 days before testing. After the designed hydration period, cylindrical pastes were crushed and sieved in two fractions, the first fraction of 2–4 mm (G) and the second fraction <0.2 mm (P). These fractions were selected to determine the factors affecting the leaching properties and, at the same time, to meet the requirements of EN 12457–2 standard, which specifies the particle size range between 0 and 4 mm. To evaluate the compositional changes in the original slag and slag pastes upon carbonation, the thermogravimetric analyses and XRD measurements were performed on these fractions after carbonation.

2.2.3.1. Carbonation. The hydrated pastes and raw BOF slag were inserted into the carbonation chamber for 3 months. The conditions for the accelerated carbonation test: 3% CO_2 and RH = 65% were chosen based on the previous studies (at these conditions, accelerated carbonation leads to similar microstructural changes and phase assemblage as observed during natural carbonation of cement pastes although the carbonation kinetics differ) [26,35]. Phenolphthalein was used as a pH indicator to estimate the carbonation depth.

2.2.3.2. Leaching of heavy metals. The tank leaching test was performed according to NEN 7375:2004 standard. It should be noted that the size of the samples ($4 \times 4 \times 4$ cm^3) was slightly below the limits specified by the standard, where the minimal size of two sample dimensions should be higher than 40 mm. Following the standard procedure, the carbonated and uncarbonated pastes were immersed in ultra-pure water (0.055 μS/cm) in sealed containers in a way that all sides were in contact with water. The eluates were exchanged periodically as specified in the standard for up to 64 days. Similarly, crushed samples and original slag were analysed before and after carbonation curing by subjecting them to the one stage batch leaching test according to EN 12457-2. The L/S ratio of 10 was applied in all cases. The samples were inserted in plastic containers with ultra-pure water and shaken for 24 h using a dynamic shaker (ES SM-30, Edmund Buhler GmbH) at a speed of 250 rpm (it must be noted that the applied speed deviates from the standard). The eluates were filtered through a 0.22 μm membrane filter, and the pH was measured with a pH meter (Volcraft) calibrated with the 2-point procedure (with the accuracy of ±0.2 pH). To determine the leaching of heavy metals, the eluates were acidified with HNO_3 and analysed with an inductively coupled plasma atomic emission spectrometer (ICP-OES, SPECTROBLUE). The cumulative release of heavy metals from the tank test (in mg per m^2) and the content of soluble components from one batch leaching test (mg per kg of dry slag) were compared with the limit values specified in the Dutch Soil Quality Decree [16].

3. Results analysis

3.1. Hydration of BOF slag phases

The early age hydration kinetics of activated BOF slag was investigated with isothermal calorimetry, as presented in Fig. 2. No substantial differences were observed between the heat flow curves of potassium and sodium citrate-activated slag, reflecting similarity in the hydration processes when these two activators are applied. After 7 days of

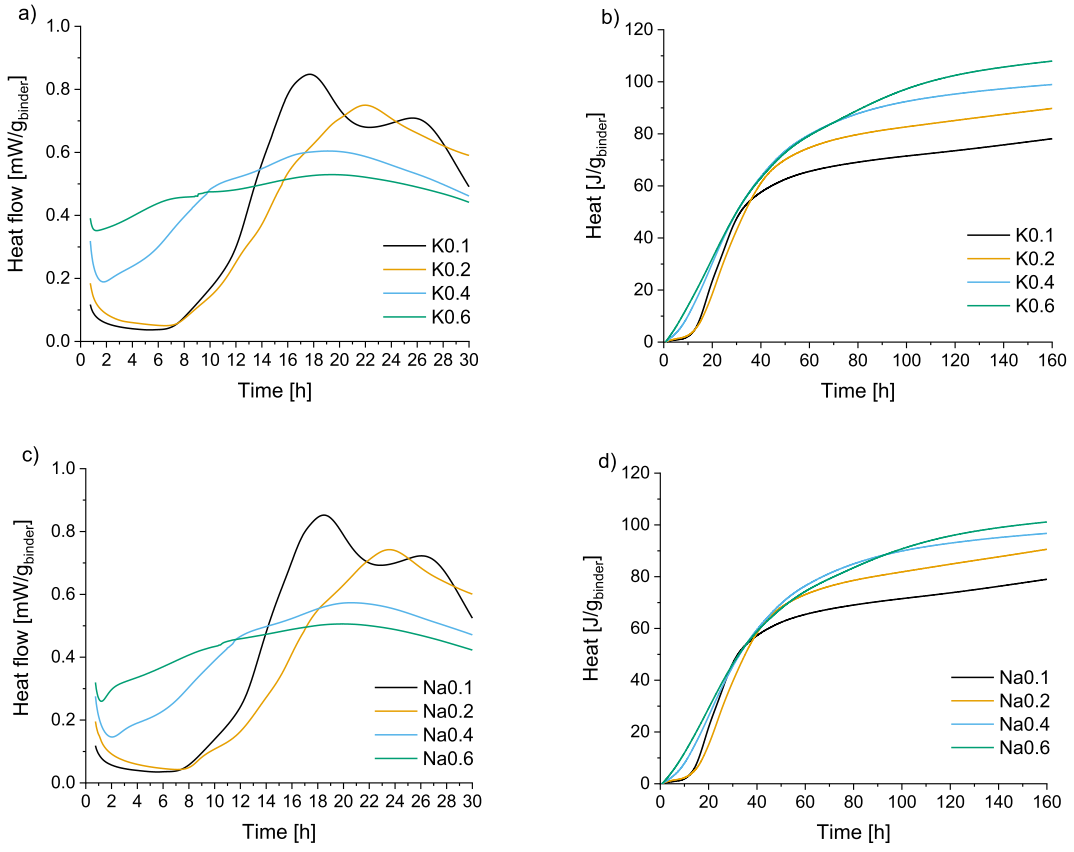

Fig. 2. Heat flow curves a),c), and cumulative heat release b), d) during hydration of BOF slag pastes.

hydration, the total heat release is slightly higher for the samples with tri-potassium citrate. In general, higher concentrations of citrate salts result in an increased amount of total heat, indicating enhanced hydration of BOF slag up to 7 days. One must note, however, that the time of heat flow maximum is greatly affected by the activator dosage, being around 18 h for 0.1 M of citrate salt, shifting towards longer times of around 22 h for 0.2 M, and being again accelerated with 0.4 and 0.6 M solutions. Moreover, with the high activator dosages (e.g. 0.4 M, 0.6 M), the broadening of the main peak and elimination of the induction period is observed. Based on these findings, it can be concluded that citrate salts act as hydration retarders at low concentrations and as accelerators at high concentrations. This behaviour was previously reported in [36].

To understand the impact of activator concentration on the dissolution of BOF slag phases and their reactivity, the solutions from pastes containing the highest and lowest activator dosage were extracted and analysed during the first hour after contact with water. The results are presented in Fig. 3 and Table 5.

Fig. 3 a) and b) shows that the concentration of all ions in the solution extracted from the BOF slag pastes at the early hydration stages drastically rises when 0.6 M solutions of citrate salts are applied in comparison to 0.1 M solutions. It is evident that with the addition of citrate salts, extraordinarily high numbers of Ca ions are released to the solution. This behaviour is in agreement with the results reported by Schwarz [37], who investigated the impact of tri-potassium citrate on cement hydration. High concentrations of iron, aluminum as well as heavy metals (chromium and vanadium) confirm the dissolution of brownmillerite at early age (see Fig. 3b). Chromium may also originate from wuestite, as magnesium and manganese are also present in the early solution with significant quantities. The dissolution of wuestite seems to be enhanced with more concentrated solutions of citrate salts. The escalated contents of multivalent cations (including aluminum, iron and magnesium) in the pore solution were previously observed in the presence of organic admixture (polycarboxylate ether) in cement pastes [38]. It must be noted that pH is also significantly altered with the variable content of citrate salts compared to the intrinsic pH of a BOF slag-water mixture of about 12.5 [3], as shown in Table 5. The higher pH values are generated in pastes with more concentrated solutions of citrate salts after 30 and 60 min of hydration.

The phase development of BOF slag pastes after selected hydration periods is presented in Fig. 4. As already indicated with the calorimetry measurements, the hydration kinetics and phase assemblage are affected by the concentration of the citrate, whereas the cation of the salt (Na vs. K) has a minor effect. Among the crystalline phases, during the first 7 days of hydration, mostly brownmillerite reacts, and the extent of the hydration of this phase is enhanced with highly concentrated citrate salts solutions. The degree of brownmillerite hydration is relatively stable at later ages. These findings are in agreement with our previous study [19]. Magnetite remains inert within the investigated hydration period, while wuestite reveals partial reactivity. The extent of hydration

Table 5
The pH of the initial citrate solutions and the solutions extracted from pastes.

Mix	pH		
	Before mixing[a]	30 min[b]	60 min[b]
K0.1	9.03	12.78	12.95
K0.6	8.99	13.41	13.29
Na0.1	8.81	12.98	12.95
Na0.6	8.56	13.79	13.62

[a] Measured.
[b] Calculated based on [OH^-].

of crystalline C_2S is similar in all pastes after 7 days of hydration, disclosing a slight tendency towards higher reaction degrees with more concentrated citrate solutions. The increased reactivity of C_2S at early hydration ages in the presence of potassium citrate was also reported in [19]. However, from the current study, it becomes evident that after 28 and 90 days, hydration of C_2S in the samples with highly concentrated citrate solutions is suppressed. In contrast, in pastes with 0.1 M and 0.2 M citrate salts, hydration of C_2S proceeds up to 90 days, reaching a hydration degree of around 50%. The main crystalline hydration product in the investigated systems is siliceous hydrogarnet, and its amount closely corresponds to the extent of brownmillerite hydration.

The differences in the reactivity of the main BOF slag phases with varying dosages of citrate activators are further reflected in the development of mechanical properties. After 7 days of hydration, the compressive strength of BOF slag pastes increases with the activator dosage. However, already the 28 days-strength values reveal the opposite tendency. After 90 days of hydration, the maximum strength of pastes with both types of the activator is reported when 0.2 M solutions are used, reaching the value of around 90 MPa. The mechanical properties closely reflect the changes in the phase composition shown in Fig. 5, emphasising the impact of belite reactivity.

3.2. Environmental impact

In order to take cognisance of physical and chemical factors affecting the leaching of heavy metals from BOF slag/slag-based materials, in this study, two methods: tank test and one batch leaching test, are employed. Additionally, in the one batch leaching test, two fractions of slag and crushed slag pastes, 0- 0.2 mm (P) and 2–4 mm (G), are investigated.

The present analyses focus on the impact of carbonation on the leaching of heavy metals from building products containing BOF slag from the perspective of carbonation-induced changes in the phase composition (and accompanying microstructural alterations) of the binder. It should be noted that the legal threshold values for the leaching of heavy metals from building products containing wastes (Soil Quality Decree [16]) in this study have indicative character since, in comparison to pastes, leaching from mortar and concrete may differ substantially.

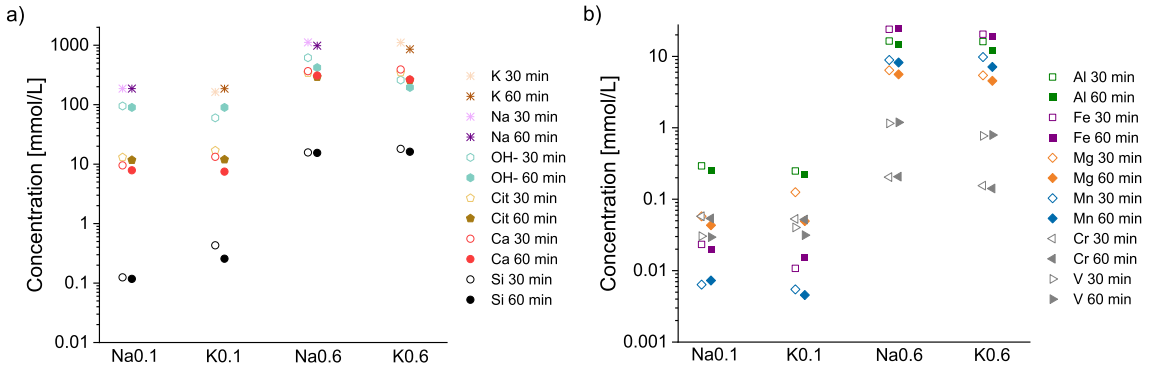

Fig. 3. The concentrations of a) high-concentration and b) low-concentration ions in the solutions extracted from pastes with 0.1 M and 0.6 M citrate salts (potassium citrate and sodium citrate).

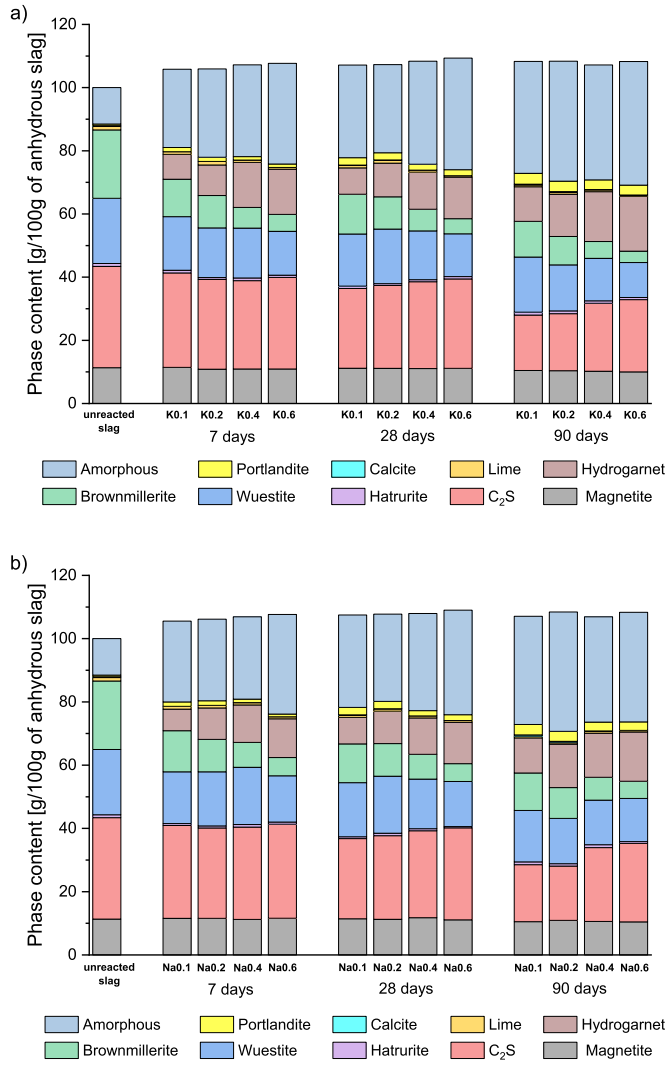

Fig. 4. Phase compositions of the BOF slag pastes after selected hydration periods (Pyroaurite is also detected, but due to its poor crystallinity and low contents, it is included in the amorphous phase).

Changes in the microstructure and transport properties induced by the presence of aggregates (e.g., due to the occurrence of interfacial transition zone) will affect the release of heavy metals. Nevertheless, the insight from this study (on the paste level) can help to isolate the factors affecting the leaching of heavy metals when mortars and concretes are investigated.

In EU, the limit values for the leaching of heavy metals are only specified for landfilling of inert wastes [39]. There is no uniform regulation concerning the leaching limits for heavy metals from building materials containing these wastes. In consequence, countries apply different testing methods and implement their own regulatory limits [40]. One batch leaching test (EN 12457-2) is commonly applied owing to its simplicity. In several countries (including France, Lithuania, Italy and Portugal), the regulatory limits of heavy metals leaching from building materials are established based on this test. In the Netherlands, the limit values refer to column leaching test, which tends to give lower leaching values in comparison to one batch leaching test (applying the same L/S ratio) [41]. However, this behaviour may differ for various materials.

In the batch leaching test, building materials are investigated in granular form (i.e. high surface area), highlighting the impact of the phase composition on the leaching of heavy metals. The data can be used to estimate the release of heavy metals at the end of concrete service life when the constructions are demolished and crushed. To account for diminished leaching from monolithic building products, in the Netherlands, tank test (NEN 7375) (with corresponding limit values in Dutch SQD) is also employed. This test is designed specifically for diffusion-controlled leaching and might be more representative for shaped products. However, it has to be noted that the release of heavy metals from building materials with different industrial wastes is often governed, next to diffusion, also by dissolution and wash-off effects [42,43], and is strongly affected by microstructural properties.

3.2.1. *Leaching of heavy metals before carbonation*

The fundamental aspects affecting the leaching behaviour from unhydrated and hydrated BOF slag concern the concentration of heavy metals and their distribution within slag phases. Regarding the slag's chemical composition (as shown in Table 1), among heavy metals, in the investigated slag, the highest concentration is reported for vanadium, followed by traces of chromium, while the scant amounts of molybdenum are below the detection limits of the XRF method. In unreacted slag, vanadium is incorporated in C_2S and brownmillerite, while chromium is detected in wuestite and brownmillerite (see Table 2). The incorporation of molybdenum is more difficult to establish due to its low contents in slag. However, it generally occurs in iron-containing phases (including brownmillerite, magnetite and wuestite) [44].

Owing to the occurrence of heavy metals in the reactive slag phases, the extent of reaction of these phases becomes crucial. As shown with the early age solution analyses, the rate of dissolution of BOF slag phases is strongly affected by the concentration of the activator. With the highly concentrated citrate solutions, considerable amounts of heavy metals are released to the solution already within the first hour of hydration. As revealed with quantitative XRD, not only the early kinetics of dissolution

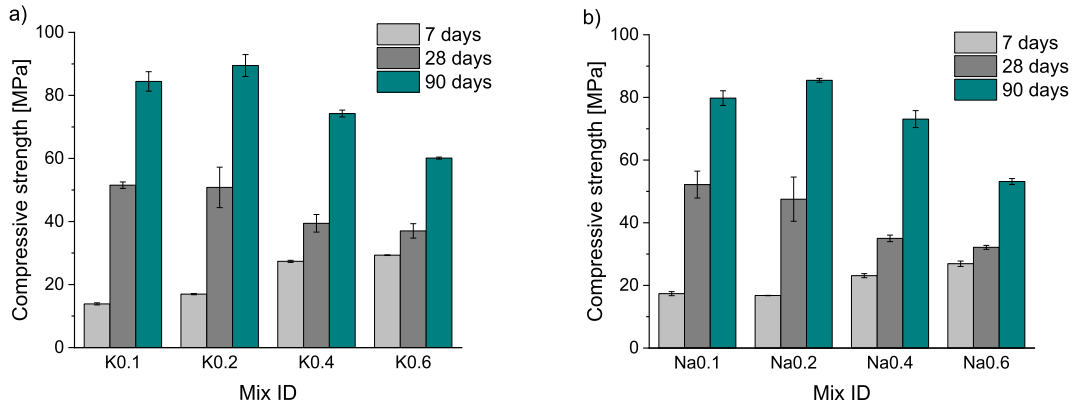

Fig. 5. Compressive strength of BOF slag pastes with a) potassium citrate and b) sodium citrate.

of slag phases but also their degree of reaction at later ages show a strong dependency on the activator dosage. Based on the reactivity of the slag phases, the greatest leaching due to brownmillerite dissolution is expected for the pastes with the highest concentrations of the activator and due to dissolution of C_2S with the concentration of 0.1 and 0.2 M potassium/sodium citrate, assuming no incorporation of heavy metals in the hydration products. Nevertheless, the immobilisation of heavy metals in the newly formed hydration products cannot be excluded, as C-S-H gel and hydrogarnets reveal high abilities to incorporate/adsorb these elements.

3.2.1.1. Vanadium. Among the trace elements in BOF slag, vanadium is often the most abundant and leachable, causing environmental issues [2,3,45]. As shown in previous research, and confirmed in this study (Fig. 6) (detailed leaching values are provided in Table a1 in Appendix A), leaching of vanadium from non-hydrated slag often exceeds the chronic toxicity thresholds [2,3]. It is generally observed that the release of vanadium is inversely proportional to the concentration of Ca^{2+} in the solution [2]. For non-hydrated BOF slag, the dependency between calcium and vanadium ions may imply that the leaching of vanadium is controlled by the $Ca_3(VO_4)_2$ solubility limits [2]. However, as shown by De Windt et al. [46], the dissolved concentrations of vanadium are too low to be exclusively governed by this mechanism. From Fig. 6 it can be seen that the leaching of vanadium intimately responds to the pH changes, being considerably reduced when pH raises from ~12 to ~13. The difference between the V leaching from the two investigated slag fractions (G and P) can be explained by the higher surface area of the finer fraction (P), which imposes greater reactivity and consequent precipitation of portlandite (pH-buffering phase). Thus, lower values of vanadium leaching are reported for the fine fraction. Similar tendencies are observed for pastes, where coarser fractions show higher leaching of vanadium, as the pH generated in eluates is lower. The leaching of vanadium from BOF slag pastes falls below the limits specified in Dutch Soil Quality Decree. At high pH, vanadium tends to form oxyanions which can be adsorbed on C-S-H gel and/or incorporated in hydrogarnet structure [2,3,22,46].

3.2.1.2. Chromium. Chromium is the second most abundant and potentially harmful heavy metal in the investigated BOF slag. The leaching of chromium from slag and slag-based pastes is presented in Fig. 7. In general, the relatively low release of chromium, not exceeding the threshold values, is observed. Among the analysed samples, the highest leaching of chromium is reported for the unhydrated slag, demonstrating a certain ability of the hydration products to immobilise chromium.

3.2.1.3. Molybdenum. Even though the total amount of molybdenum in BOF slag is insignificant, the leaching of molybdenum is analysed in this study since brownmillerite (most likely the hosting phase of molybdenum) reveals high reactivity in the presented systems [44]. Fig. 8 shows the leaching of molybdenum from unhydrated and hydrated BOF slag. For all samples, the leaching falls far below the SQD limits. Nevertheless, the tendency towards a higher release from the pastes with an increasing concentration of activator can be observed.

3.2.2. Leaching of heavy metals after carbonation

Upon carbonation, the original BOF slag phases, as well as the hydration products, are destabilised, and therefore, the adsorbed/incorporated heavy metals can be released. In order to reveal the impact of carbonation on the compositional changes in original and hydrated slag, a comparison between the carbonated powders (<0.2 mm) and non-carbonated samples (unreacted slag and pastes after 90 days of hydration) is made in Fig. 9. The results demonstrate that in unhydrated BOF slag, C_2S is prone to carbonation (with the reaction degree of about 25%), while other phases are relatively inert. These findings agree well with the reports on post-carbonation leaching from BOF slags presented in the literature [2,3]. In carbonated BOF slag, aragonite is identified as the main carbonation product.

Similar tendencies are observed for the hydrated slag samples, where C_2S partially undergoes carbonation (up to 15%), while wuestite and brownmillerite remain inert. Among the hydration products, upon carbonation, portlandite is almost entirely consumed, and about 75% of hydrogarnet is decomposed. The exact reaction of hydrogarnet decomposition, however, requires further investigation, as no crystalline Fe-strätlingite or iron hydroxide could be identified with the XRD method. In contrast to the non-hydrated BOF slag, the carbonation of pastes results in the formation of vaterite and calcite. According to Auroy et al. [47], the presence of vaterite is a characteristic for the carbonation of C-S-H gel at accelerated carbonation conditions (3% of CO_2). Since the largest vaterite quantities are observed for the samples activated with 0.1 and 0.2 M citrate solutions, where the highest degree of C_2S reaction is observed, the presence of vaterite likely corresponds to the carbonation of C-S-H gel in our study. The carbonation of C-S-H gel is confirmed with experiments and thermodynamic modeling in many previous studies [48–50]. The differences between the carbonates formed in the samples with varying activator dosage are further reflected with thermogravimetric analyses (Fig. 10). In order to account for the mass contribution of citrate, the graphs are corrected by subtracting the mass loss from the non-carbonated corresponding pastes (Fig. 10, insert). In general, in all samples, carbonates decompose in the broad temperature range (between 500 and 800 °C). However, the mass loss is shifted towards lower temperatures for the samples with less concentrated citrate solutions, indicating differences in the physical

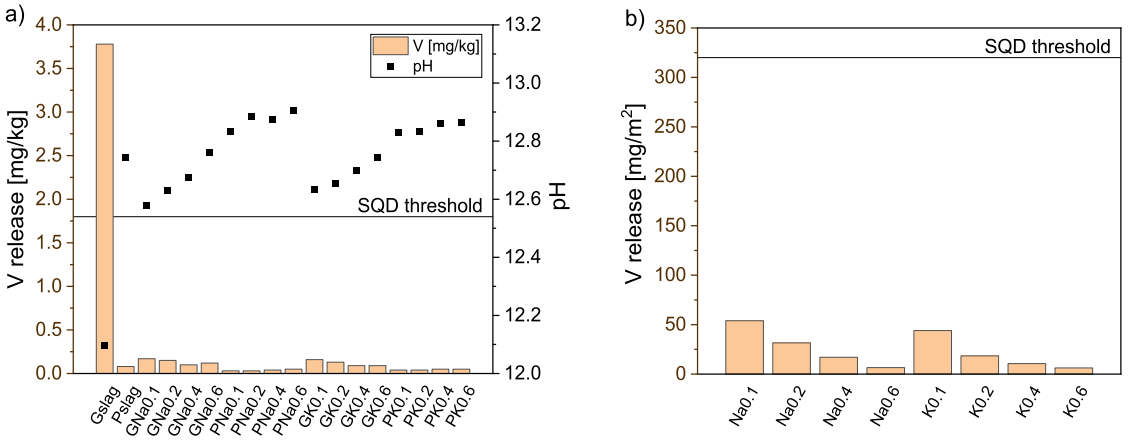

Fig. 6. Leaching of vanadium before carbonation, derived from a) one batch test, b) tank test (G refers to 2–4 mm size fraction, P to <0.2 mm).

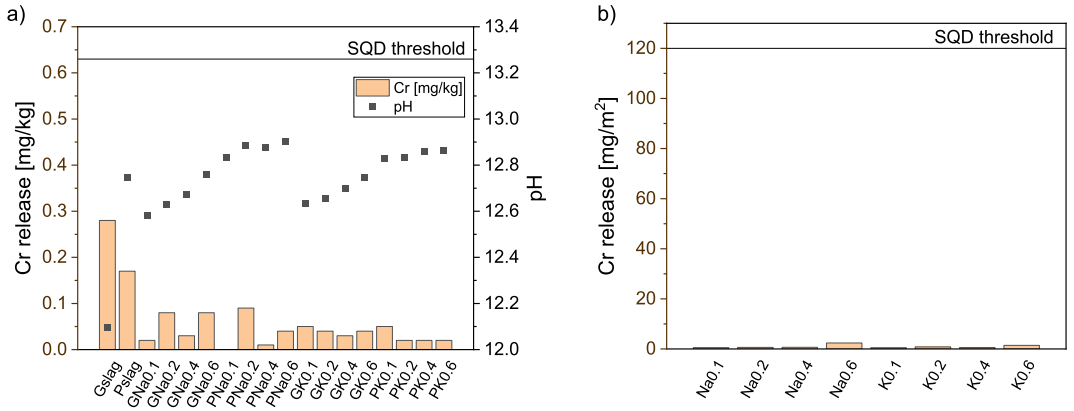

Fig. 7. Leaching of chromium before carbonation, derived from a) one batch test, b) tank test.

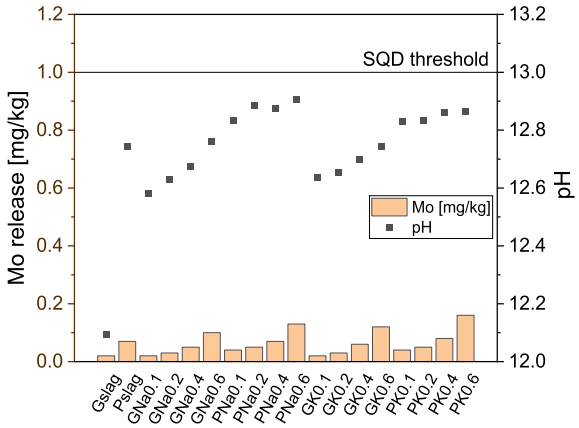

Fig. 8. Leaching of molybdenum before carbonation, derived from one batch test (the results from the tank test are not shown due to very limited concentrations).

properties of carbonates formed [51].

The post-carbonation leaching, especially of shaped slag-based materials is not exclusively a result of the destabilisation of phases but a compilation of several simultaneous effects. For example, the resistance of the material to carbonation must be considered. As shown in Table 6, with the phenolphthalein test, no substantial extent of carbonation is detected for all samples. One of the reasons for the limited carbonation depth is the very dense microstructure, i.e. low porosity [19]. Only the tendency towards a higher carbonation depth with an increasing activator dosage (up to 1.5 mm for slag activated with 0.6 M solutions) is observed. While for the powder fraction, the amount of carbonates derived from the thermogravimetric method noticeably decreases with the increasing activator dosage (Table 6), for the 2–4 mm fraction, the differences in the carbonates content are significantly diminished. This might be associated with the varying carbonation depths in 2–4 mm grains which tend to increase for samples with more concentrated citrate solutions. Several factors affecting the quantity of carbonates, their physical nature, and carbonation depth can be distinguished.

On the one hand, taking into account the activator dosage, higher resistance to carbonation could be expected with more concentrated activators, assuming the increased content of Na^+/K^+ in the pore solution, and hence a larger alkalinity buffer [52]. On the other hand, in samples with a lower activator dosage, the degree of C_2S hydration is higher, implying a denser microstructure (further supported by better mechanical performance), which impedes the CO_2 ingress. Furthermore, larger quantities of portlandite in these samples result in the volume increase and formation of a dense protective layer of carbonates on the surface of the sample upon carbonation [49,51,53]. In contrast, during the carbonation of the C-S-H gel, coarsening of the microstructure might occur, especially with a low Ca/Si ratio, facilitating the CO_2 ingress [53,54]. Phase analyses also demonstrate that hydration products are more prone to carbonation than the original slag phases. This might explain the larger quantities of carbonates in the powdered samples with less concentrated citrate solutions resulting from the reaction of C-S-H gel with CO_2.

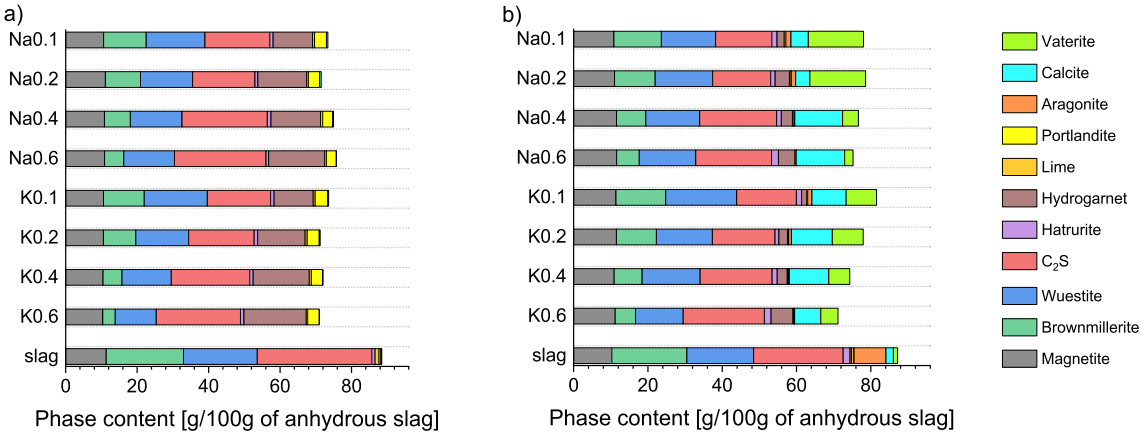

Fig. 9. Crystalline phase composition of slag/slag pastes a) after 90 days of hydration, b) after 90 days of hydration and subsequent 90 days of carbonation (powder samples <0.2 mm).

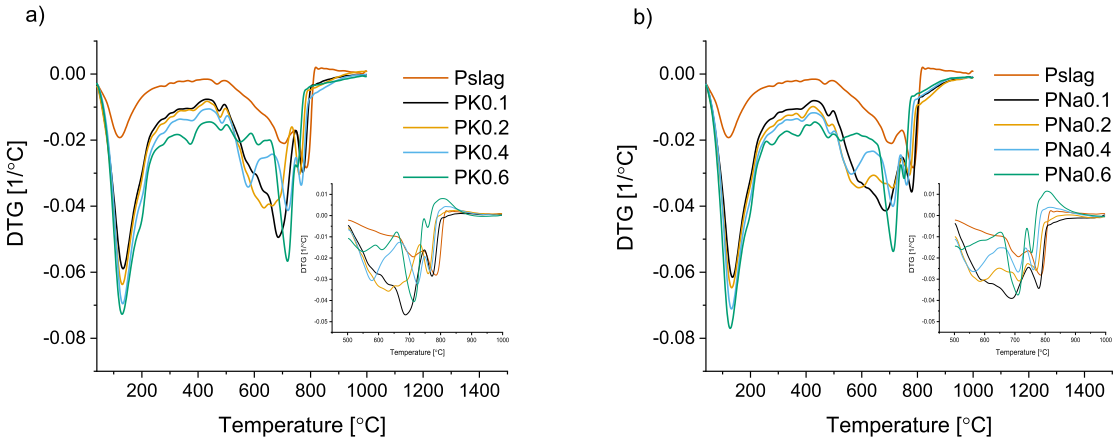

Fig. 10. DTG curves of carbonated slag/slag pastes analysed on the <0.2 mm fraction. The inserted graphs show the decomposition of carbonates in the temperature range between 500 and 1000 °C, after correcting for citrate mass loss.

Table 6
The mass losses due to carbonate decomposition determined with thermogravimetry and carbonation depths measured with phenolphthalein test.

Parameter		Slag	K0.1	K0.2	K0.4	K0.6	Na0.1	Na0.2	Na0.4	Na0.6
Mass loss 500–800 °C [%]	<0.2 mm	3.7	7.8	6.9	5.7	4.2	8.3	7.3	5.5	4.0
	2–4 mm	0.2	5.5	6.0	4.9	3.9	5.9	4.0	5.1	4.0
Carbonation depth [mm]	2–4 mm	0	0.5	0.5	1	1.5	0.5	0.5	1	1.5

3.2.2.1. Vanadium. After carbonation, the leaching of vanadium increases significantly, exceeding the legal thresholds in the one batch leaching test up to 100 times (Fig. 11). In the tank test, however, where the impact of carbonation depth plays a crucial role, the BOF slag pastes meet the leaching standards defined in SQD. The strong correlation between vanadium leaching and the extent of carbonation is especially visible when comparing the two fractions of slag/pastes. Powder samples show several times higher leaching than the samples with 2–4 mm grain size, implying that the ratio between carbonated and non-carbonated sections defines the magnitude of vanadium leaching. Even though the pH of eluates from the samples with highly concentrated citrate salts is more alkaline, the release of vanadium is boosted in these samples, likely due to the greater carbonation depth and decomposition of hydrogarnets (Fig. 9).

3.2.2.2. Chromium. The leaching of chromium from plain BOF slag after carbonation is not considerably affected, remaining below the restrictive levels, which agrees with the study by Huijgen and Comans [55]. In contrast, the chromium release from the crushed, carbonated, citrate activated pastes is significantly increased, especially in pastes with 0.6 M potassium/sodium citrate solutions. This behaviour can be the consequence of the highest reactivity of brownmillerite and partial reactivity of wuestite (which contain Cr) in these samples and destabilisation of their hydration products upon carbonation, as revealed with the phase analysis (Fig. 9). The presence of citrate complexes with chromium and their decomposition with the pH drop also cannot be excluded. The tank test (Fig. 12), however, clearly demonstrates that from the shaped products, where carbonation depth is insubstantial, the leachability of chromium is very limited. The presented data indicate that too high concentrations of citrate activator can result in the boost of chromium leaching, and this phenomenon must be considered when designing BOF slag-based materials in engineering practice.

3.2.2.3. Molybdenum. The leaching of molybdenum from plain BOF slag shows only a slight increase after carbonation (Fig. 13). This behaviour contradicts the results of Baciocchi [56], who reported a decreased release of Mo after carbonation. In the study of Costa [17], where two slags with varying composition were analysed, after carbonation, for one slag, Mo leaching was reduced and for another slag, it increased. In one batch leaching test, the release of molybdenum from

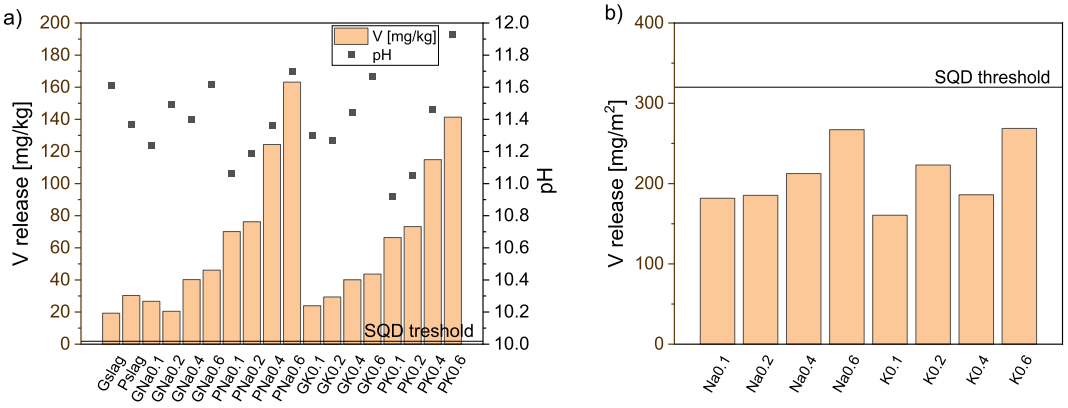

Fig. 11. Leaching of vanadium after carbonation derived from a) one batch test, b) tank test.

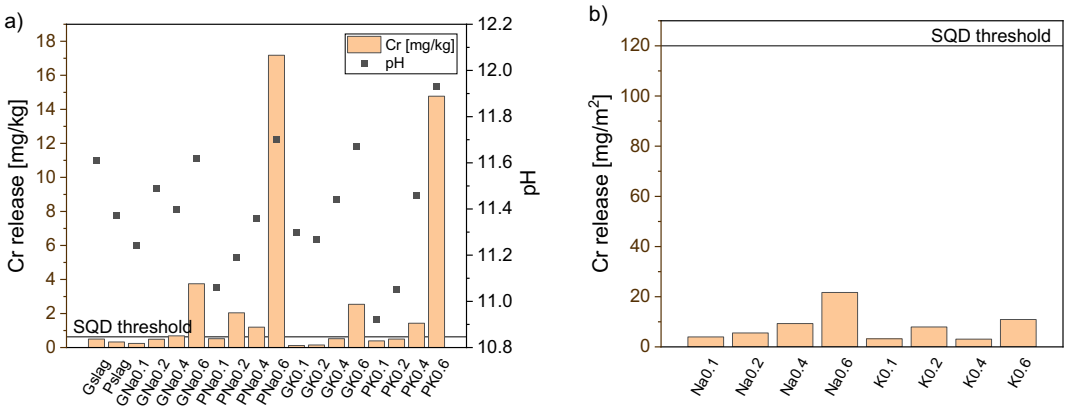

Fig. 12. Leaching of chromium after carbonation, derived from a) one batch test, b) tank test.

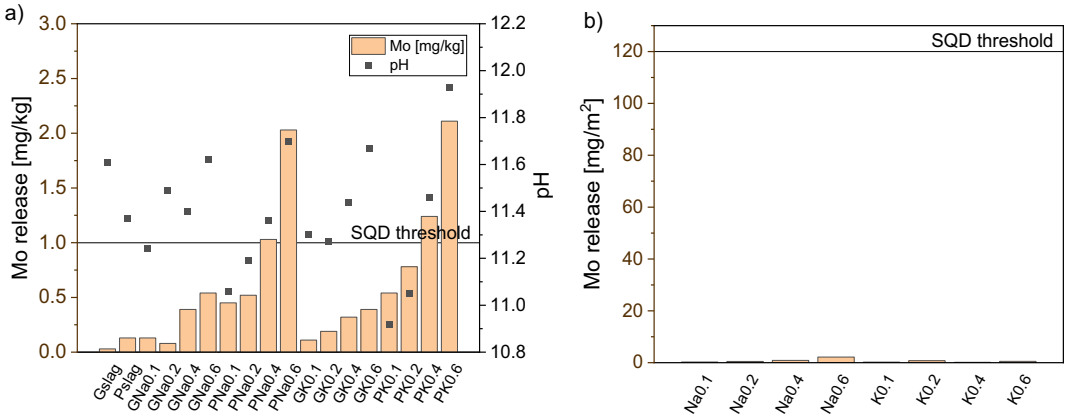

Fig. 13. Leaching of molybdenum after carbonation, derived from a) one batch test, b) tank test.

the carbonated samples escalates, exceeding the threshold values for samples with the highest activator dosages. As shown with the phase analyses of carbonated and non-carbonated materials (Fig. 9), brownmillerite (Mo hosting phase) is much more stable upon carbonation than its hydration products. In consequence, the highest leaching of molybdenum is observed for the samples with the greatest extent of brownmillerite hydration. Even though after carbonation, molybdenum becomes very mobile in the carbonated areas, considering its content in slag and carbonation resistance of pastes, the leaching of molybdenum is not a restraining factor for the application of slag products, as confirmed with the tank test.

4. Conclusions

Chemically activated BOF slag pastes are the newly-designed potential building products. To assess the risk of environmental harmfulness of these materials during their service life, in this paper, the leaching of heavy metals upon carbonation is investigated. Potassium and sodium citrate salts are used with variable dosages to activate slag with the aim to provide a comprehensive overview of the impact of the hydration degree of BOF slag phases on the leaching behaviour of pastes. The carbonation resistance of BOF slag/slag pastes and the compositional changes induced by carbonation are assessed. To examine the effects of physical and chemical changes, which occur simultaneously upon carbonation, the leaching of heavy metals is determined with the tank test and one batch leaching test on shaped and unshaped materials (fractions <0.2 mm and 2–4 mm), respectively. The following conclusions are reached within this study.

- The hydration kinetics of BOF slag phases can be controlled and optimised with the addition of potassium/sodium citrate. Whereas the type of activator has a minor impact on the hydration kinetics and phase development, the dosage of the activator is pivotal. At the early hydration ages, the reactivity of BOF slag phases, especially of brownmillerite, is accelerated by the highly concentrated solutions. Siliceous hydrogarnets and C-S-H gel are formed. However, the high concentrations of activators adversely affect the long-term strength development due to the suppressed reaction of C_2S in these pastes.
- Even though reactions of most contaminated phases take place, the leaching of heavy metals (including vanadium, chromium and molybdenum) from hydrated BOF slag is insubstantial. The release of vanadium (the most abundant heavy metal) from non-carbonated pastes closely corresponds to the pH changes, being significantly diminished at pH close to 13.
- After 90 days of sealed curing, BOF slag pastes reveal high resistance to carbonation. In consequence, the release of heavy metals in the tank leaching test, where the leachability is mostly determined by the carbonation depth, does not exceed the legal thresholds specified in Soil Quality Decree. In one batch leaching test, the general tendency towards intensified heavy metal leaching from the pastes with highly concentrated citrate solutions is observed. This can be associated with the greatest degree of brownmillerite hydration in these samples and the decomposition of its reaction product- hydrogarnet, which potentially hosts heavy metals in the hydrated slag. As the immobilisation capability of BOF slag hydrates drastically drops upon carbonation, the carbonation resistance (depth of carbonation) becomes crucial in preventing the release of heavy metals from BOF slag-based products. This study demonstrates that the resistance to

carbonation can be improved by facilitating the hydration of C_2S in the BOF slag with the use of low concentrations of citrate salts (e.g. 0.1 M and 0.2 M in this study).

CRediT authorship contribution statement

A.M. Kaja: Conceptualization; Methodology; Investigation; Data curation; Formal analysis; writing-original draft.

A. Delsing: Investigation.

S.R. van der Laan: Writing – Review Editing.

H.J.H. Brouwers: Funding acquisition; Supervision, Writing – Review Editing.

Qingliang Yu: Conceptualization; Funding acquisition; Supervision, Writing – Review Editing.

Declaration of competing interest

The authors declare that they have no known competing financial interests or personal relationships that could have appeared to influence the work reported in this paper.

Acknowledgment

The authors would like to acknowledge the financial support by NWO (The Netherlands Organisation for Scientific Research) for funding this research (project no. 12824). Special thanks are given to Marco Rijnders for performing the EPMA measurements.

Appendix A

Table a1
Leaching values of heavy metals from BOF slag/slag pastes in one batch and tank leaching test.

Sample	One batch leaching test							
	Leaching before carbonation				Leaching after carbonation			
	V	Cr	Mo	pH	V	Cr	Mo	pH
	[mg/kg]	[mg/kg]	[mg/kg]	[−]	[mg/kg]	[mg/kg]	[mg/kg]	[−]
Gslag	3.78	0.28	0.02	12.10	19.29	0.5	0.03	11.61
Pslag	0.08	0.17	0.07	12.75	30.31	0.33	0.13	11.37
GNa0.1	0.17	0.02	0.02	12.58	26.67	0.24	0.13	11.24
GNa0.2	0.15	0.08	0.03	12.63	20.49	0.49	0.08	11.49
GNa0.4	0.1	0.03	0.05	12.68	40.22	0.69	0.39	11.4
GNa0.6	0.12	0.08	0.1	12.76	46.1	3.75	0.54	11.62
PNa0.1	0.03	0	0.04	12.84	70.1	0.52	0.45	11.06
PNa0.2	0.03	0.09	0.05	12.89	76.2	2.04	0.52	11.19
PNa0.4	0.04	0.01	0.07	12.88	124.35	1.2	1.03	11.36
PNa0.6	0.05	0.04	0.13	12.91	163.21	17.18	2.03	11.7
GK0.1	0.16	0.05	0.02	12.64	23.9	0.12	0.11	11.3
GK0.2	0.13	0.04	0.03	12.66	29.42	0.15	0.19	11.27
GK0.4	0.09	0.03	0.06	12.70	40.07	0.52	0.32	11.44
GK0.6	0.09	0.04	0.12	12.75	43.68	2.54	0.39	11.67
PK0.1	0.04	0.05	0.04	12.83	66.38	0.39	0.54	10.92
PK0.2	0.04	0.02	0.05	12.84	73.24	0.5	0.78	11.05
PK0.4	0.05	0.02	0.08	12.86	114.88	1.43	1.24	11.46
PK0.6	0.05	0.02	0.16	12.87	141.35	14.77	2.11	11.93

Sample	Tank test					
	Leaching before carbonation			Leaching after carbonation		
	V	Cr	Mo	V	Cr	Mo
	[mg/m^2]	[mg/m^2]	[mg/m^2]	[mg/m^2]	[mg/m^2]	[mg/m^2]
Na0.1	53.92	0.50	bdl	181.73	3.97	0.25
Na0.2	31.60	0.64	bdl	185.35	5.55	0.48
Na0.4	17.03	0.66	bdl	212.51	9.30	0.89
Na0.6	6.53	2.38	0.78	267.14	21.70	2.15
K0.1	44.02	0.48	bdl	160.58	3.23	0.21
K0.2	18.40	0.80	bdl	223.16	7.95	0.78
K0.4	10.59	0.55	bdl	186.04	3.07	0.14
K0.6	6.19	1.42	0.55	268.68	10.93	0.50

References

[1] Mineral Commodity Summaries 2019: U.S. Geological Survey vol. 3, U.S. Geological Survey, 2019.
[2] A.J. Hobson, et al., Mechanism of vanadium leaching during surface weathering of basic oxygen furnace steel slag blocks: a microfocus X-ray absorption spectroscopy and Electron microscopy study, Environ. Sci. Technol. 51 (2017) 7823–7830, https://doi.org/10.1021/acs.est.7b00874.
[3] A. van Zomeren, S.R. van der Laan, H.B.A. Kobesen, W.J.J. Huijgen, R.N. J. Comans, Changes in mineralogical and leaching properties of converter steel slag resulting from accelerated carbonation at low CO2 pressure, Waste Manag. 31 (2011) 2236–2244, https://doi.org/10.1016/j.wasman.2011.05.022.
[4] S.Z. Carvalho, F. Vernilli, B. Almeida, M. Demarco, S.N. Silva, The recycling effect of BOF slag in the portland cement properties, Resour. Conserv. Recycl. 127 (September) (2017) 216–220, https://doi.org/10.1016/j.resconrec.2017.08.021.
[5] F. Han, Z. Zhang, D. Wang, P. Yan, Hydration heat evolution and kinetics of blended cement containing steel slag at different temperatures, Thermochim. Acta 605 (2015) 43–51, https://doi.org/10.1016/j.tca.2015.02.018.
[6] B. Das, S. Prakash, P.S.R. Reddy, V.N. Misra, An overview of utilization of slag and sludge from steel industries, Resour. Conserv. Recycl. 50 (2007) 40–57, https://doi.org/10.1016/j.resconrec.2006.05.008.

[7] F. Han, Z. Zhang, Properties of 5-year-old concrete containing steel slag powder, Powder Technol. 334 (2018) 27–35, https://doi.org/10.1016/j.powtec.2018.04.054.

[8] J. Li, Q. Yu, J. Wei, T. Zhang, Structural characteristics and hydration kinetics of modified steel slag, Cem. Concr. Res. 41 (2011) 324–329, https://doi.org/10.1016/j.cemconres.2010.11.018.

[9] C. van Hoek, J. Small, S. van der Laan, Large-area phase mapping using PhAse recognition and characterization (PARC) software, Micros. Today 24 (2016) 12–21, https://doi.org/10.1017/S1551929516000572.

[10] A. M. Kaja and Q. L. Yu, "Method for the manufacture of high-end performance steel slag-based building products, U.S. Provisional Pat. Ser. No. 62/821603, filed 3/21/2019".

[11] Q. Zhao, C. Liu, L. Cao, X. Zheng, M. Jiang, Effect of lime on stability of chromium in stainless steel slag, Minerals 8 (2018) 1–10, https://doi.org/10.3390/min8100424.

[12] P. Chaurand, et al., Environmental impacts of steel slag reused in road construction: a crystallographic and molecular (XANES) approach, J. Hazard. Mater. 139 (2007) 537–542, https://doi.org/10.1016/j.jhazmat.2006.02.060.

[13] J.F.P. Gomes, C.G. Pinto, Leaching of heavy metals from steelmaking slags, Rev. Metal. 42 (6) (2006), https://doi.org/10.3989/revmetalm.2006.v42.i6.39.

[14] U.V. Oty, Steel Slag Leachates : Environmental Risks and Metal Recovery Opportunities, University of Hull, 2015.

[15] P. Chaurand, J. Rose, J. Domas, J.Y. Bottero, Speciation of Cr and V within BOF steel slag reused in road constructions, J. Geochem. Explor. 88 (SPEC. ISS) (2006) 10–14, https://doi.org/10.1016/j.gexplo.2005.08.006.

[16] "Soil Quality Decree," 2015. http://wetten.overheid.nl/BWBR0023085/2015-07-01#BijlageA (accessed Jul. 19, 2018).

[17] G. Costa, A. Polettini, R. Pomi, A. Stramazzo, Leaching modelling of slurry-phase carbonated steel slag, J. Hazard. Mater. 302 (2016) 415–425, https://doi.org/10.1016/j.jhazmat.2015.10.005.

[18] H. Preßlinger, K.O. Klepp, Vanadium in converter slags, Steel Res. 73 (2002) 522–525, https://doi.org/10.1002/srin.200200022.

[19] A.M. Kaja, S. Melzer, S. van der Laan, H.J.H. Brouwers, Q.L. Yu, Hydration of potassium citrate-activated BOF slag, Cem. Concr. Res. 140 (2021) 106291.

[20] I. Moulin, J. Rose, W. Stone, J. Bottero, Lead, zinc and chromium (III) and (VI) speciation in hydrated cement phases, Waste Mater. Constr. (2000) 269–280.

[21] S. Hillier, D.G. Lumsdon, R. Brydson, E. Paterson, Hydrogarnet: a host phase for Cr (VI) in chromite ore processing residue (COPR) and other high pH wastes, Environ. Sci. Technol. 41 (2007) 1921–1927, https://doi.org/10.1021/es0621997.

[22] A. Vollpracht, W. Brameshuber, Binding and leaching of trace elements in Portland cement pastes, Cem. Concr. Res. 79 (2016) 76–92, https://doi.org/10.1016/j.cemconres.2015.08.002.

[23] M.L.D. Gougar, B.E. Scheetz, D.M. Roy, Ettringite and C-S-H Portland cement phases for waste ion immobilization: a review, Waste Manag. 16 (1996) 295–303, https://doi.org/10.1016/S0956-053X(96)00072-4.

[24] O.E. Omotoso, D.G. Ivey, R. Mikula, Characterization of chromium doped tricalcium silicate using SEM/EDS, XRD and FTIR, J. Hazard. Mater. 42 (1995) 87–102, https://doi.org/10.1016/0304-3894(95)00012-J.

[25] A. Polettini, R. Pomi, P. Sirini, Fractional factorial design to investigate the influence of heavy metals and anions on acid neutralization behavior of cement-based products, Environ. Sci. Technol. 36 (2002) 1584–1591, https://doi.org/10.1021/es010002z.

[26] M. Castellote, L. Fernandez, C. Andrade, C. Alonso, Chemical changes and phase analysis of OPC pastes carbonated at different CO2 concentrations, Mater. Struct. Constr. 42 (2009) 515–525, https://doi.org/10.1617/s11527-008-9399-1.

[27] T.F. Sevelsted, J. Skibsted, Carbonation of C-S-H and C-A-S-H samples studied by 13C, 27Al and 29Si MAS NMR spectroscopy, Cem. Concr. Res. 71 (2015) 56–65, https://doi.org/10.1016/j.cemconres.2015.01.019.

[28] K. De Weerdt, G. Plusquellec, A. Belda Revert, M.R. Geiker, B. Lothenbach, Effect of carbonation on the pore solution of mortar, Cem. Concr. Res. 118 (2019) 38–56, https://doi.org/10.1016/j.cemconres.2019.02.004.

[29] V. Morin, P. Termkhajornkit, B. Huet, G. Pham, Impact of quantity of anhydrite, water to binder ratio, fineness on kinetics and phase assemblage of belite-ye'elimite-ferrite cement, Cem. Concr. Res. 99 (2017) 8–17, https://doi.org/10.1016/j.cemconres.2017.04.014.

[30] Y. Zuo, M. Nedeljković, G. Ye, Pore solution composition of alkali-activated slag/fly ash pastes, Cem. Concr. Res. 115 (2019) 230–250, https://doi.org/10.1016/j.cemconres.2018.10.010.

[31] D. Jansen, F. Goetz-Neunhoeffer, C. Stabler, J. Neubauer, A remastered external standard method applied to the quantification of early OPC hydration, Cem. Concr. Res. 41 (2011) 602–608, https://doi.org/10.1016/j.cemconres.2011.03.004.

[32] BS-EN-196-1. Methods of testing cement – Part 1: determination of strength, Br. Stand. Institution-BSI CEN Eur. Comm. Stand. (2005), https://doi.org/10.1111/j.1748-720X.1990.tb01123.x.

[33] "EA NEN 7375:2004 - Leaching characteristics of moulded or monolithic building and waste materials", 2005.

[34] D. Laerke Baun, J. Holm, J. B. Hansen, and M. Wahlström, "CEN EN 12457 leaching test," 2003. [Online]. Available: http://www.nordtest.org/register/techn/tlibrary/tec539.pdf.

[35] M. Auroy, et al., Comparison between natural and accelerated carbonation (3% CO2): impact on mineralogy, microstructure, water retention and cracking, Cem. Concr. Res. 109 (2018) 64–80, https://doi.org/10.1016/j.cemconres.2018.04.012.

[36] J. T. Pacanovsky, L. Huang, T. Frank, and M. Samy, "Hydration control of cementitious systems," 1996, [Online]. Available: https://patents.google.com/patent/US5634972A/en.

[37] W. Schwarz, Novel cement matrices by accelerated hydration of the ferrite phase in Portland cement via chemical activation: kinetics and cementitious properties, Adv. Cem. Based Mater. 2 (1995) 189–200, https://doi.org/10.1016/1065-7355(95)90003-9.

[38] F. Caruso, S. Mantellato, M. Palacios, R.J. Flatt, ICP-OES method for the characterization of cement pore solutions and their modification by polycarboxylate-based superplasticizers, Cem. Concr. Res. 91 (2017) 52–60, https://doi.org/10.1016/j.cemconres.2016.10.007.

[39] Council of the European Union, "Council decision of 19 December 2002 establishing criteria and procedures for the acceptance of waste at landfills pursuant to Article 16 of and Annex II to Directive 1999/31/EC," Off. J. Eur. Communities, pp. 27–49, 2003.

[40] D. Blasenbauer, et al., Legal situation and current practice of waste incineration bottom ash utilisation in Europe, Waste Manag. 102 (2020) 868–883, https://doi.org/10.1016/j.wasman.2019.11.031.

[41] M.J. Quina, J.C.M. Bordado, R.M. Quinta-Ferreira, Percolation and batch leaching tests to assess release of inorganic pollutants from municipal solid waste incinerator residues, Waste Manag. 31 (2) (2011) 236–245, https://doi.org/10.1016/j.wasman.2010.10.015.

[42] K. Mizerna, A. Krol, Leaching of heavy metals from monolithic waste, Environ. Prot. Eng. 44 (4) (2018) 143–158, https://doi.org/10.5277/epel80410.

[43] C. Lampris, J.A. Stegemann, M. Pellizon-Birelli, G.D. Fowler, C.R. Cheeseman, Metal leaching from monolithic stabilised/solidified air pollution control residues, J. Hazard. Mater. 185 (2–3) (2011) 1115–1123, https://doi.org/10.1016/j.jhazmat.2010.10.021.

[44] M. Spanka, T. Mansfeldt, R. Bialucha, Sequential extraction of chromium, molybdenum, and vanadium in basic oxygen furnace slags, Environ. Sci. Pollut. Res. 25 (2018) 23082–23090, https://doi.org/10.1007/s11356-018-2361-z.

[45] A.J. Hobson, D.I. Stewart, R.J.G. Mortimer, W.M. Mayes, M. Rogerson, I.T. Burke, Leaching behaviour of co-disposed steel making wastes : effects of aeration on leachate chemistry and vanadium mobilisation, Waste Manag. 81 (2018) 1–10, https://doi.org/10.1016/j.wasman.2018.09.046.

[46] L. De Windt, P. Chaurand, J. Rose, Kinetics of steel slag leaching: batch tests and modeling, Waste Manag. 31 (2011) 225–235, https://doi.org/10.1016/j.wasman.2010.05.018.

[47] M. Auroy, et al., Comparison between natural and accelerated carbonation (3% CO2): impact on mineralogy, microstructure, water retention and cracking, Cem. Concr. Res. 109 (2018) 64–80, https://doi.org/10.1016/j.cemconres.2018.04.012.

[48] A. Morandeau, M. Thiéry, P. Dangla, Cement and concrete research impact of accelerated carbonation on OPC cement paste blended with fl y ash, Cem. Concr. Res. 67 (2015) 226–236, https://doi.org/10.1016/j.cemconres.2014.10.003.

[49] V. Shah, K. Scrivener, B. Bhattacharjee, S. Bishnoi, Changes in microstructure characteristics of cement paste on carbonation, Cem. Concr. Res. 109 (2018) 184–197, https://doi.org/10.1016/j.cemconres.2018.04.016.

[50] Z. Shi, et al., Experimental studies and thermodynamic modeling of the carbonation of Portland cement, metakaolin and limestone mortars, Cem. Concr. Res. 88 (2016) 60–72, https://doi.org/10.1016/j.cemconres.2016.06.006.

[51] H. Justnes, J. Skocek, T.A. Østnor, C.J. Engelsen, O. Skjølsvold, Microstructural changes of hydrated cement blended with fly ash upon carbonation, Cem. Concr. Res. 137 (2020) 106192, https://doi.org/10.1016/j.cemconres.2020.106192.

[52] M. Nedeljković, B. Ghiassi, S. van der Laan, Z. Li, G. Ye, Effect of curing conditions on the pore solution and carbonation resistance of alkali-activated fly ash and slag pastes, Cem. Concr. Res. 116 (2019) 146–158, https://doi.org/10.1016/j.cemconres.2018.11.011.

[53] A.M. Kaja, H.J.H. Brouwers, Q.L. Yu, NOx degradation by photocatalytic mortars: The underlying role of the CH and C-S-H carbonation, Cem. Concr. Res. 125 (2019), https://doi.org/10.1016/j.cemconres.2019.105805.

[54] A. Morandeau, M. Thiéry, P. Dangla, Impact of accelerated carbonation on OPC cement paste blended with fly ash, Cem. Concr. Res. 67 (2015) 226–236, https://doi.org/10.1016/j.cemconres.2014.10.003.

[55] W.J.J. Huijgen, Carbonation of Steel Slag for CO2 Sequestration: Leaching of Products and Reaction Mechanisms 40, 2006, pp. 2790–2796, https://doi.org/10.1021/es052534b.

[56] R. Baciocchi, G. Costa, A. Polettini, R. Pomi, Effects of thin-film accelerated carbonation on steel slag leaching, J. Hazard. Mater. 286 (2015) 369–378, https://doi.org/10.1016/j.jhazmat.2014.12.059.